

Combined SMOS and SMAP sea ice thickness Arctic

This document is a modified version of the deliverable D6.3 of the Horizon2020 project SPICES

Authors:

Amelie Schmitt, University of Hamburg

Lars Kaleschke, Max-Planck-Institute of Meteorology

1 Introduction

We present data sets of sea ice thickness derived from brightness temperatures (TBs) from the passive microwave sensors flying onboard the Soil Moisture and Ocean Salinity (SMOS) and the recently launched Soil Moisture Active Passive (SMAP) satellites.

We apply the sea ice thickness retrieval algorithm by Tian-Kunze et al. (2014) - which was developed for brightness temperatures near-nadir - and adapt it to the SMAP incidence angle of 40°. In the following sections we briefly summarize the retrieval algorithm and describe the sea ice thickness data set produced in the framework of SPICES.

2 Sea ice thickness retrieval algorithm

The sea ice thickness retrieval is based on L-band brightness temperature intensities. We use the gridded TB datasets from SMOS and SMAP at an incidence angle of 40°, which are described in more detail in Schmitt and Kaleschke (2018).

We adapt the retrieval algorithm by Tian-Kunze et al. (2014), which is currently in operational use at the University of Hamburg to produce daily Arctic sea ice thickness maps from SMOS data at near-nadir incidence angles. Here, we only briefly summarize the most important aspects of the algorithm and refer to the original publication for more details. The algorithm was adapted to the SMAP incidence angle of 40°. Furthermore, due to improvements of the computation times we were able to implement the retrieval as a forward model instead of the iterative approach used by Tian-Kunze et al. (2014).

2.1 Retrieval model

The sea ice radiation model used for the retrieval is adapted from Menashi et al. (1993). It consists of a single plane sea ice layer bordered by the underlying sea water and the air on top. The brightness temperatures depend on the bulk temperature (T_i) and the bulk emissivity (ϵ) of the sea ice layer:

$$TB = \epsilon(d_{ice}, V_b, \theta) \cdot T_i,$$

where the emissivity depends mainly on the ice thickness (d_{ice}), but also on brine volume (V_b) and incidence angle (θ). The brine volume is a function of ice temperature and ice salinity (S_i) (Cox and Weeks, 1983).

Using an empirical function of Rynlin (1974) the ice salinity can be estimated from the ice thickness and the salinity of the underlying sea water. A monthly climatology of sea surface salinity is used for the computations.

Since the radiation model does not include a snow layer we neglect the impact of snow on the L-band emission. However, the insulation effect of snow is accounted for in the thermodynamic model used to calculate bulk sea ice temperatures. We apply a one-dimensional thermodynamic model based on Maykut (1986), which consists of one sea ice layer with a snow layer on top. T_i is calculated from the incoming and outgoing fluxes at the surface that are assumed to compensate each other. The fluxes are calculated using 2-m air temperature and 10-m wind speed fields from the Japanese reanalysis (JRA).

2.2 Saturation and maximum retrievable thickness

Assuming a homogeneous, plane sea ice layer over the L-band sensor footprint, measured brightness temperatures increase non-linearly with increasing sea ice thickness (Figure 1) due to the limited penetration depth of L-band radiation. The sensitivity is largest for thin ice while TBs saturate for thicknesses larger than a certain thickness d_{max} . As in Tian-Kunze et al. (2014) we define d_{max} as the point where the TB change per ice thickness increment falls below 0.1K per cm.

In the sea ice thickness product, we indicate saturation by the saturation ratio, which is calculated as $100\% d_{ice}/d_{max}$. For a saturation ratio of 100% the actual thickness is not known. It can only be inferred that $d_{ice} \geq d_{max}$ and thus these cases should be handled with care or discarded completely, depending on the application.

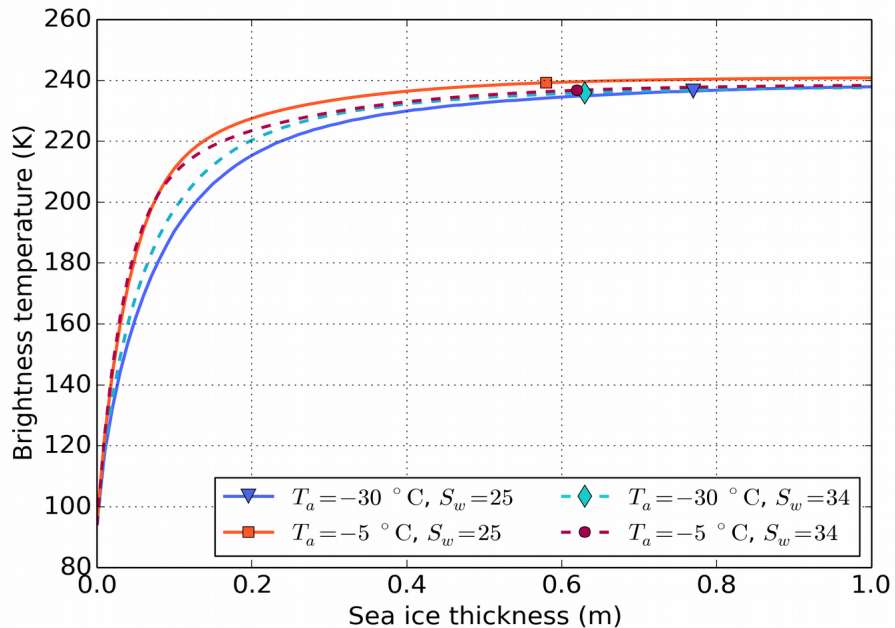


Figure 1 Brightness temperatures as function of sea ice thickness for different combinations of constant air temperatures (T_a) and water salinities (S_w) during polar night with a wind speed of 5m/s. The symbols mark the maximum retrievable thickness.

The maximum retrievable thickness does not only depend on sea ice temperature and salinity but also on incidence angle (Figure 2). The penetration depth is largest for cold ice with a low salinity. d_{max} also decreases with increasing incidence angle. The difference between nadir (Tian-Kunze et al., 2014) and 40° (this product) can be up to 8% for cold conditions.

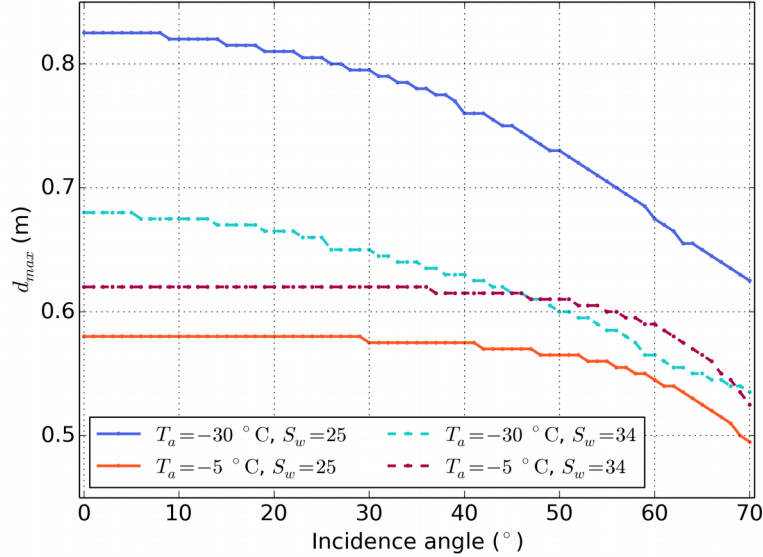


Figure 2 d_{max} as function of incidence angle for different combinations of constant air temperatures (T_a) and water salinities (S_w) during polar night with a wind speed of 5m/s.

2.3 Ice thickness distribution (post-processing)

In reality, ice thicknesses are usually not homogeneous within a sensor footprint of about 40 km. We account for the errors caused by the plane ice layer assumption using a post-processing approach, which accounts for the subpixel-scale heterogeneity of the ice thickness. As in Tian-Kunze et al. (2014) we assume that the ice thickness distribution is lognormal $p(d_{ice}, \mu, \sigma)$ with a constant value of $\sigma = 0.6$, which was derived from NASA's Operation IceBridge data. μ is determined from the measured TB data at every grid point using a least-squares method. TBs are calculated for every ice thickness up to 4m, weighted by the lognormal distribution and integrated over the whole thickness range to correct for the impact of the ice thickness distribution.

2.4 Uncertainty assessment

There are many different sources of uncertainty that may influence the ice thickness retrieval. It remains difficult to estimate the combined impact of different uncertainty sources. A general estimation of possible uncertainties caused by different sources is given in Tian-Kunze et al. (2014). They discuss the impact of model assumptions, such as the assumption of 100% sea ice concentration, uncertainties of the estimated sea ice temperatures and salinity, as well as uncertainties of the assumptions about the shape of the ice thickness distribution.

In this product, we only calculate the ice thickness uncertainties caused by TB uncertainties. The TB uncertainties given in the SMOS and SMAP TB products are used to calculate a possible ice thickness range. An illustration of the calculated uncertainties is given in Figure 3. It is evident that a constant TB standard error causes a smaller thickness error for thin ice and a larger thickness error for thicker ice. In addition, the ice thickness uncertainty interval is asymmetric with larger uncertainty values for larger ice thicknesses.

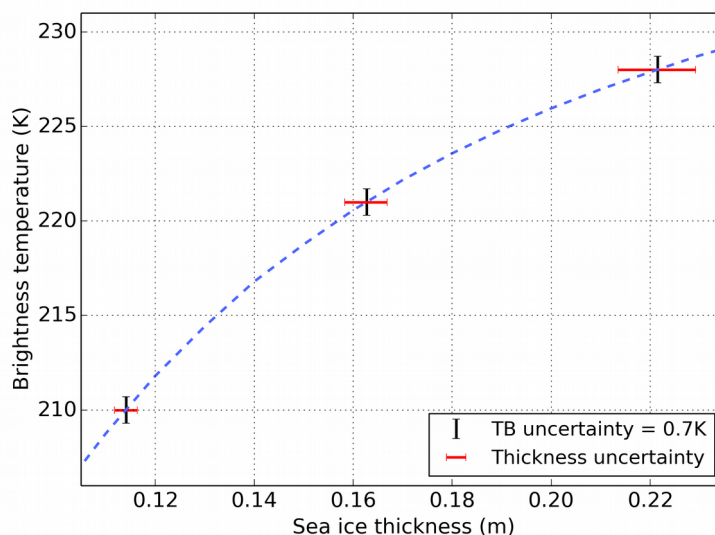


Figure 3 Sea ice thickness uncertainty intervals calculated using a constant TB uncertainty of 0.7 K.

3 Gridded datasets

An overview of the variables in the file is given in Table 1. The files contain sea ice thickness and the corresponding uncertainty intervals. Due to the limited penetration depth of L-band radiation in melting sea ice, ice thicknesses are only calculated during the freeze-up period between 15 October and 15 April.

Table 1 Variable names and description.

Variable name	Variable description
time	Time since 1 January 2010
TB_intensity	Brightness temperature intensity at an incidence angle of 40°
plane_layer_thickness	Sea ice thickness using the plane layer assumption
sea_ice_thickness	Sea ice thickness with post-processing to account for the sea ice thickness distribution
thickness_uncertainty_upper	Upper limit of the sea ice thickness uncertainty interval
thickness_uncertainty_lower	Lower limit of the sea ice thickness uncertainty interval
saturation_ratio	Saturation ratio: Ratio of plane layer thickness and maximum retrievable thickness

We provide thicknesses calculated using combined TBs from SMOS and SMAP. A major advantage of the combined thickness product is the better spatial coverage in lower latitudes or when single swaths of one of the sensors are corrupted or missing. To obtain a homogenized TB product we apply a bias correction to the polarized TBs from SMAP. It was already demonstrated by Schmitt and Kaleschke (2018) that a linear fit with time constant parameters is suitable for this purpose. We apply the following bias corrections:

$$TB_{v,corr} = 1.021 TB_{v,SMAP} - 3.997$$

$$TB_{h,corr} = 0.987 TB_{h,SMAP} + 7.533$$

For the combined product, TB intensities and the corresponding uncertainties from SMOS and SMAP are averaged at every grid point.

4 Acronyms

Acronym	Definition
EASE grid	Equal-Area Scalable Earth grid
JRA	Japanese Reanalysis
SMAP	Soil Moisture Active Passive satellite
SMOS	Soil Moisture and Ocean Salinity satellite
TB	Brightness temperature

5 References

G. Cox, and W. Weeks (1983): Equations for determining the gas and brine volumes in sea-ice samples. *J. Glaciol.*, 29, 306-316. doi=10.1017/S0022143000008364

G. A. Maykut (1986): *Geophysics of Sea Ice*, chap. The surface heat and mass balance, 395-463, Plenum, New York.

J. Menashi, K. Germain, C. Swift, J. Comiso, and A. Lohanick (1993): Low-frequency passive-microwave observations of sea ice in the Weddell Sea. *J. Geophys. Res.*, 98, 22569-22577. doi=10.1029/93JC02058

A. I. Ryvlin (1974): Method of forecasting flexural strength of an ice cover. *Probl. Arct. Antarct.*, 45, 79-86.

Schmitt, A. U. and Kaleschke, L. (2018). A Consistent Combination of Brightness Temperatures from SMOS and SMAP over Polar Oceans for Sea Ice Applications. *Remote Sensing*, 10(4), 553. doi: <https://doi.org/10.3390/rs10040553>

X. Tian-Kunze, L. Kaleschke, N. Maaß, M. Mäkynen, N. Serra, M. Drusch, and T. Krumpfen (2014): SMOS-derived thin sea ice thickness: algorithm baseline, product specifications and initial verification. *The Cryosphere*, 8, 997-1018. doi=10.5194/tc-8-997-2014